catalysis

Structural characterization of W-Ni-Al$_2$O$_3$ catalysts

M.H. Jordão,[a] J.M. Assaf,[a] P.A.P. Nascente[b] and V.R. Mastelaro[c*]

[a]DEQ-UFSCar, C.P. 676, São Carlos S.P. Brazil
[b]CCDM-DEMa-UFSCar, São Carlos - S.P., Brazil
[c]IFSC-USP São Carlos - C.P. 369 - S.P., Brazil
valmor@if.sc.usp.br

A series of W/Ni/Al$_2$O$_3$ catalysts was prepared by coprecipitation of nickel and aluminum and impregnation of tungsten. The samples were characterized by XRD, XPS and XAS techniques. XRD measurements detected two phases: NiO as the main phase and NiAl$_2$O$_4$ in lower amount; no phase containing tungsten was detected. XPS measurements indicated the presence of Al$_2$O$_3$, NiAl$_2$O$_4$, and Al$_2$(WO$_4$)$_3$ phases on the catalyst surfaces. The XANES spectra of catalysts were rather similar for all of the samples. According to the EXAFS results, at the short range level, tungsten does not form any bound with Ni atoms. The six nickel first coordination shell in the catalysts containing tungsten is similar to that encountered in COP 1 catalyst without tungsten. The lower Ni-Ni coordination number observed for all catalysts, when compared to the NiO phase, can be attributed to the nickel-aluminum interaction.

Keywords: catalysts, W-Ni-Al$_2$O$_3$, XAS, XPS, structure

1. Introduction

W-Ni-alumina catalyst are applied to several industrial chemical reactions, such as hydrogenation, steam reforming of hydrocarbons and in hydrodessulfurization (Thomas et al., 1982 and Scheffer et al., 1987). W promoted coprecipitated Ni-alumina catalyst have been studied in steam reforming of hydrocarbons, in which tungsten plays a fundamental role in the selectivity of some reactions (Bonneau et al., 1991 and Zielinski, 1993).

In this work we have investigated the influence of tungsten on the structure of catalysts of nickel/tungsten supported on alumina by X-Ray Diffraction (XRD), X-Ray Photoelectron Spectroscopy (XPS) and X-Ray Absorption Spectroscopy (XAS).

2- Experimental

The method used in the preparation of the W/Ni/Al$_2$O$_3$ catalysts, designated here as COP, was the coprecipitation of nickel and aluminum hydroxicarbonates from their nitrates, followed by calcination to obtain Ni and Al oxides and impregnation of tungsten (Narayanan et al., 1995). The coprecipitation was carried out at pH 8.0 and 60 ^{o}C, using sodium carbonate as precipitate agent. The material was washed until sodium had been eliminated, dried, and calcined in synthetic air at 500°C. Then tungsten was impregnated, with excess of solvent, from silicotungstic acid. The nickel/aluminum ratio was kept constant, and the nominal amounts of tungsten (wt%) were 0.0 (COP 1), 2.5 (COP 2), 9.5 (COP 3) and 15,5 (COP 4). The quantities of Ni, Al and W in the resulting oxides were determined by inductively coupled plasma spectroscopy (ICP) and atomic absorption spectroscopy (AAS). ICP and AAS analyses were performed using a Thermo Jarrel Ash (AtomScan 25) and an Intralab (AA 1475) spectrometers, respectively. The

phase identification was done by X-ray diffraction (XRD) using a Carl Zeiss Jena (URD6) diffractometer. The determination of the atomic ratios and the identification of the oxidation states were carried out by XPS using a Kratos XSAM HS spectrometer. The experiments were performed in ultra-high vacuum (low 10^{-7} Pa range) using Mg Kα (hv = 1253.6 eV) X-ray source operated at 15 kV and 15 mA. The binding energies were referenced to adventitious carbon 1s line set at 284.8 eV.

Ni K-edge EXAFS spectra were collected at the Brazilian Synchrotron Light Source Laboratory (LNLS) using the XAS beam line. The LNLS storage ring was operated at 1.36 GeV and 80-120 mA. Data were collected at the Ni K-edge (8333 eV) in a transmission mode using a Si (111) channel-cut monochromator. Ionization chambers were used to detect the incident and transmitted flux. An energy steps equal to 1.0 and 2.0 eV were respectively used to collect the data at XANES and EXAFS regions of the absorption edge. The energy calibration of the monochromator was checked after each spectrum using a Ni metal foil to provide good energy reproducibility.

Polycrystalline NiO sample was used as reference to obtain structural information concerning the Ni-O and Ni-Ni bonds in the analyzed samples. In NiO, each Ni atom is surrounded by six oxygen atoms situated at an average distance of 2.09 Å and 12 Ni atoms are situated at 2.95 Å (Sasaki et al., 1979).

The K edge EXAFS and XANES spectra were analyzed by subtracting a linear background computed by least-square fitting from the pre-edge region. All XANES spectra were normalized by the maximum K edge peak. The EXAFS oscillation curves were obtained by a standard procedure (Konisberger and Prins, 1988), normalized, background removed, and Fourier transformed using the available Winxas program (Resller, 1997). The Fourier transform was obtained after a k^2 EXAFS weighting and a Bessel apodization function (coefficient of 4) was applied over 2.2 to 12.2 Å^{-1}.The errors were estimated to be ± 0.01 Å (± 0.02 Å) in the distance, ± 5% (10%) in the coordination number and in the Debye-Waller factor for the first oxygen and first nickel contributions respectively. The reliability of the fit was determined by the residual parameter χ_v^2 (Lytle et al., 1989).

3- Results and Discussion

The concentrations (weight percentages) obtained by ICP and AAS are presented in Table I.

Table I. Ni/Al ratios and W amounts (in weight %) determined by ICP and AAS.

Sample	Ni/Al Ratio	W
COP 1	3.20	0
COP 2	3.25	2.4
COP 3	3.25	8.8
COP 4	3.27	13.9

According to the results obtained by ICP and AAS, the Ni/Al ratios in the catalysts are constant and the amounts of W are slightly lower than the nominal ones.

XRD results show that the catalyst precursor has hydrotalcite-type structure, and indicate a mixture of two crystalline phases, NiO and NiAl$_2$O$_4$. For all samples, NiO is the main phase. No metallic W or a phase containing this metal was detected by XRD.

The XPS results for the binding energies and atomic ratios are presented in Table II and Table III, respectively.

Table II. Binding energies (eV) for the COP catalysts.

Catalyst	Binding Energy (eV)		
	Al 2p	Ni $2p_{3/2}$	W $4f_{7/2}$
COP 1	75.0	856.5	—
COP 2	75.4	857.1	36.9
COP 3	75.2	856.8	36.6

Table III. Atomic ratios for the COP catalysts.

Catalyst	Ni/Al	W/Al	W/Ni
COP 1	0.43	—	—
COP 2	0.56	0.029	0.052
COP 3	0.50	0.088	0.17

The binding energy values of Ni $2p_{3/2}$ are consistent with $NiAl_2O_4$, but not with NiO. So, we can conclude that NiO, detected by XRD, is present on the catalyst bulk. W $4f_{7/2}$ binding energies can be associated with $Al_2(WO_4)_3$. The values of Al 2p are in accordance with that of Al_2O_3, $Al_2(WO_4)_3$ and $NiAl_2O_4$ compounds The atomic ratios shown in Table III indicate that Ni and Al ions are distributed evenly, but the addition of a small quantity of tungsten causes a competition between Ni and W ions with Al ions, resulting in the surface segregation of Ni ions and/or the formation of species containing Al-W. The decrease in the Ni surface concentration as the amount of W increases indicates that tungsten coating is forming on nickel.

XANES spectra at the Ni K edge of the analyzed samples is compared with the XANES spectra of NiO in Figure 1, and their shapes are rather similar for all samples.
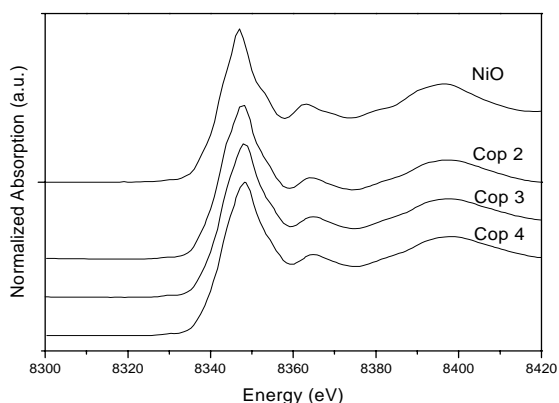

Figure 1. XANES spectra at the Ni K edge of the samples NiO, COP 2, COP 3 and COP 4

The experimental EXAFS spectra $k^2\chi(k)$ at the Ni K edge for the studied catalyst are shown in Figure 2. For the sake of comparison, the EXAFS function corresponding to NiO is also included. The EXAFS spectra of the catalysts closely resemble that of the reference NiO. From the data of Figure 2, one main aspect is noteworthy: there is a qualitative decrease in the intensity of the $k^2\chi(k)$ function, for the high values of k, with respect to the pure NiO. However, it seems that the increasing of tungsten content did not introduce any expressive change in the catalyst short-range structure. The same behavior was also observed by XRD.
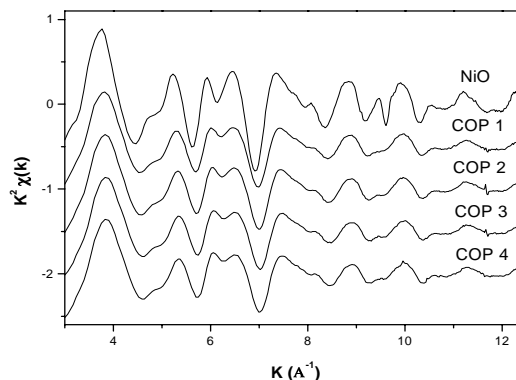
Figure 2. EXAFS spectra $k\chi(k)$ at the Ni K edge for the samples: NiO, COP 1, COP 2, COP 3 and COP 4.

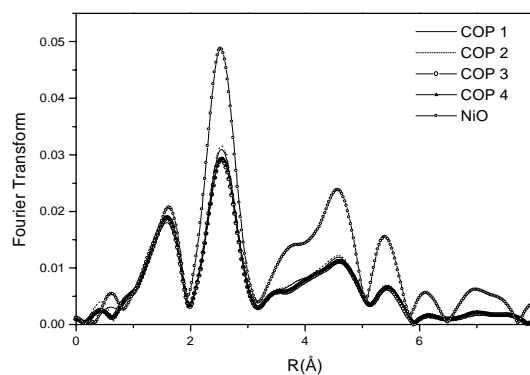The Fourier transforms (FTs) obtained from the EXAFS spectra presented in Figure 2 are show in Figure 3.

Figure 3. Fourier transforms for the samples: NiO, COP 1 COP 2, COP 3 and COP 4.

The FTs are not correct for phase shift parameters, so that the maximum peak positions are shifted to lower values compared to the real one. The FT obtained for NiO shows maxima at 1.57, 2.50, 3.72, 4.56 and 5.37 Å, corresponding to Ni-O and Ni-Ni scatter pairs placed in successive coordination shells. The first maximum (1.57 Å) corresponds to the first coordination shell, composed of six oxygen atoms. The second maximum (2.50 Å) is mainly related to the second shell consisting of 12 nickel atoms. The third and forth maximum (3.72 and 4.56 Å in the figure 3) consist of oxygen atoms (8 oxygen atoms) and nickel and oxygen atoms (8 nickel and 24 oxygen atoms), respectively. Finally, the fifth maximum located at 5.37 Å is associated with 18 Ni atoms. As it can be observed in the EXAFS spectra of these samples, there is a significative difference between NiO and the analyzed catalysts. However, little difference among the catalyst samples is observed with the increase of tungsten content. Due to the complexity of shells located at a distance higher than 3 Å, we will limit our fitting to the first and second shells (Ni-O and Ni-Ni pairs).

To obtain the best fit, we were obliged to simulate the first and the second coordination shells simultaneously. The Ni-O and Ni-Ni shells contribution were isolated by Fourier filtering of the spectra between 0.8 and 3.16 Å. The information about Ni-O and

Ni-Ni bonds was obtained by lest square fitting of the k-weighted filtered spectra in the range $2.5 < k < 12.2$ Å^{-1}, using the Ni-O and Ni-Ni backscattering amplitudes and phase shifts extract from the NiO EXAFS spectrum, taken as a reference compound. The obtained fitting parameters are summarized in Table IV. As an example, the agreement between the filtered EXAFS spectra and fitted curve for the COP 1 and COP 4 samples are presented in Figure 4. The fitting quality are the practically the same for all others samples.
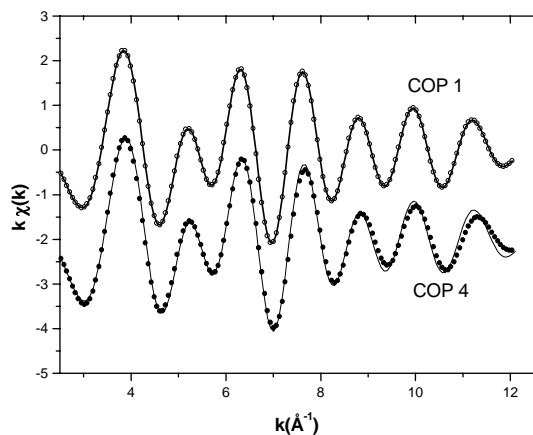

Figure 4. EXAFS spectra and fitted curve for the COP 1 and COP 4 samples

Table IV- EXAFS parameters of the first oxygen and nickel coordination shells for the studied catalyst. N is the coordination number, R is interatomic Ni-O and Ni-Ni distances, σ^2 is the absolute Debye-Waller factor and χ_v^2 is the fitting residual parameter.

Sample	N_{Ni-O}	R_{Ni-O} (Å)	σ^2_{Ni-O} (Å^2) x10^{-3}	N_{Ni-Ni}	R_{Ni-Ni} (Å)	σ^2_{Ni-Ni} (Å^2) x10^{-3}	χ_v^2
c-NiO*	6.0	2.09	-----	12	2.95	----	----
COP 1	6.1	2.07	2.0	7.9	2.95	1.0	0.5
COP 2	5.9	2.07	1.2	8.2	2.95	0.4	0.7
COP 3	6.0	2.07	1.3	8.0	2.95	1.5	0.5
Cop 4	6.0	2.06	1.5	8.2	2.94	1.7	1.2

(according to Sasaki et al., 1979).

According to Table IV, at the first Ni-O coordination shell, the nickel coordination number in the catalysts containing tungsten is similar to that found in COP 1 catalyst without tungsten. The Ni-O mean bond length in the catalysts is similar. The small difference in the first peak intensity of the Fourier transform is taken into account by the Debye-Waller factor, σ, which is related to the thermal and topological disorders.

The second shell around nickel atoms in the catalysts is composed only by nickel atoms. According to the results presented in Table IV, the Ni-Ni neighbor's number in the catalysts did not change with tungsten amount increase, being equal to the catalyst without tungsten (COP 1 sample). Thus, no interaction between nickel and tungsten atoms was observed, even for the catalyst containing 15,5 weight % of tungsten. The lower Ni-Ni coordination number observed for all catalysts, when compared to the NiO phase, can be attributed to the nickel-aluminum interaction.

4- Concluding remarks

XRD measurements identified only a mixture of NiO and $NiAl_2O_4$ phases for coprecipitated catalysts; NiO is the main phase. No crystalline structure involving W atoms was detected.

XPS results indicated the presence of $NiAl_2O_4$, Al_2O_3 and $Al_2(WO_4)_3$ on the catalyst surfaces with different amounts of W. No NiO phase was detected by XPS.

According to the EXAFS results, at the short range level, tungsten does not form any bound with Ni. The Ni first coordination shell in the catalysts containing tungsten is similar to that encountered in COP 1 catalyst without tungsten. The lower Ni-Ni coordination number observed for all catalysts, when compared to the NiO phase, can be attributed to the nickel-aluminum interaction.

5- References

Bonneau L., Arnaout K., and Duprez D., (1991). *Applied Catalysis.* **74**, 173-190.

Konisberger D.C. and Prins R., (1988). *X-Ray Absorption Techniques of EXAFS, SEXAFS and XANES* (Wiley, New York).

Lytle F.W., Sayers D.E. and Stern E.A., (1989) *Physica B* 158, 701-722.

Thomas R., Van Oers E. M., de Beer V. H. J., Medema J. and Moulijn J. A., (1982). .*Journal of Catalysis,* **76**, 241-253.

Mangnus P. J., Bos A. and Moulijn J. A, (1994). *Journal of Catalysis,* **146**, 437-448.

Narayanan S., Unnikrishnan R. and Vishwanathan V., (1995). *Applied Catalysis A: General*, **129**, 9-19.

Resller T., (1997). *J. Phys. IV* (7), C2-269-272.

Sasaki S., Fugino K., Takeuchi Y., (1979). *Proceedings of the Japan Academy* 55, 43-45.

Scheffer B., Heijeinga J. J. and Moulijn J. A., (1987) *J. Phys. Chem.* **91**, 4752-4759.

Singh V.K. and Chetal A.R., (1993*). X-Ray Spectrometry*, Vol. 22, 86-88.

Zielinski J., (1993) *Applied Catalysis A General*, **94**, 107-115.